Scale-up And Production Of Uranium-bearing QC Reference Particulates By An Aerosol Synthesis Method

Spencer M. Scott[1], Aaron T. Baldwin[1], Michael G. Bronikowski[1], Michael A. DeVore II[1], Laken A. Inabinet[1], Wendy W. Kuhne[1], Benjamin E. Naes[2], Ross J. Smith[1], Eliel Villa-Aleman[1], Travis J. Tenner[2], Kimberly N. Wurth[2], Matthew S. Wellons[1]

[1] Savannah River National Laboratory, Aiken SC
[2] Los Alamos National Laboratory, Los Alamos NM

1 Abstract

The International Atomic Energy Agency (IAEA) requires actinide-containing reference particulates for use in quality control (QC) proficiency swipe testing applications to support the international network of analytical laboratories. The QC particle products must be uniform in physical characteristics and produced at milligram-scale to ensure enough material quantities for repeated periodic use. To meet these needs, an aerosol-based method to manufacture monodisperse QC particulate actinide materials for IAEA safeguards analysis applications in the requisite milligram-scale quantities was developed. This capability was realized through the development of the Monodisperse Particle Production and Collection System (MPPaCS), which utilizes a liquid-to-particle aerosol-based technique to fabricate particles with controllable size, material phase, and isotopic composition. The MPPaCS combines a commercial aerosol generator, in-line process monitoring instrumentation, and electrostatic collection to aggregate particulates in the form of flowable powders. Scale-up engineering involved examination of production efficiency, tuning of production parameters, and characterization of products using microanalytical methods. Sustained milligram-scale particle production required multi-day continuous operations to produce monodisperse uranium particulates with an average diameter near 1-μm and a geometric standard deviation (GSD) less than 1.15. Production rates were approximately 0.33 mg per hour and batches of 5-10 milligrams each were generated. Among several uranium solution feedstocks tested, uranyl oxalate demonstrated the most useful drying dynamics to facilitate monodispersed particle size populations and spherical morphologies. The resultant products are a primarily an oxalate phase as characterized by Raman spectroscopy and have a calculated density of approximately 3.1 g/cm^3 via in-situ aerodynamic particle size spectrometer measurements. Particles generated with two deplete uranium feedstock isotopic compositions were analyzed by secondary ion mass spectrometry to characterize and confirm interparticle isotopic homogeneity. Future efforts will be focused on the inclusion and development of in-line heating components to allow thermal conversion of oxalate feedstocks into oxide particulates.

2 Introduction

Particle characterization of environmental samples for safeguards purposes conducted by the IAEA Network of Analytical Laboratories (NWAL) requires periodic application of QC. Environmental swipe samples collected by IAEA inspectors from within a nuclear facility site are subjected to two common forms of measurement: (1) a total destructive bulk analysis which consumes the entire sample and (2) analysis of particles of interest on a swipe substrate. Both measurement regimes require fit-for-purpose reference particulates with tailored isotopic, elemental, and morphological properties.[1] The QC materials for particle analysis are extremely difficult to produce in quantities sufficient to support manufacture of swipe-type samples and for the high quantities required for NWAL QC activities over multi-year periods.[2] Suitable QC particle production technologies must generate milligram-scale materials with physical and chemical characteristic uniformities in dimensions, monodispersion on wafers and/or planchets, inter-particle elemental and isotopic composition, and morphology.

Current actinide QC particle synthesis routes are divided between hydrothermal chemical reaction routes and aerosol-based generation technologies. These two strategies are complimentary across a variety of technical facets, but in general terms, hydrothermal methods are readily scalable for production throughput and aerosol-based methods are easily tuned for particle size and monodispersion manipulation. Both methods have enjoyed sustained R&D by various IAEA member state support programs in an effort to advance the respective technologies to an IAEA-qualified operational status. Within the past decade teams from the US Support Program led by Pacific Northwest National Laboratory and a multiagency European Union team associated with the French Alternative Energies and Atomic Energy Commission (CEA) have pursued R&D on hydrothermal methods.[3, 4] Parallel efforts focused on aerosol-based methods include teams from the US Support Program led by Savannah River National Laboratory and separately with

the European Commission Joint Research Centre (JRC) in collaboration with the Forschungszentrum Jülich (FZJ, Juelich/Germany) Support Program.[5-8] The JRC/FZJ collaboration has resulted in a qualified QC particle generation capability and routinely generates batches of nanogram scale uranium-laden QC reference samples, but does not currently generate QC reference particulates on the milligram scale.[9]

SRNL has focused on scale-up operations for aerosol-based uranium-containing QC reference particulate materials and has now demonstrated this capability as a complete MPPaCS. This platform, which is a combination of commercial instrumentation and SRNL-engineered tools including a robust aerosol generator, automated inline QC monitoring, and an electrostatic collector for product collection and aggregation, scales up production capability from nanograms to milligrams. Monodisperse aerosol generators are inherently limited by low feedstock injection rates, but the MPPaCS has demonstrated routine particle population size distribution stability over tens-of-hour durations, which enables the sustained operations needed to reach milligram production aliquots. QC reference particles to date are uranyl oxalate phase with tunable particle sizes of typically 0.8-1.2 µm in diameter, GSD <1.15, and with depleted uranium (DU) isotopic compositions. Test particulates have been characterized by aerodynamic particle sizing, automated electron microscopy methods, X-ray diffraction, micro-Raman spectroscopy, and large geometry secondary ion mass spectrometry (LG-SIMS). In this paper, two different DU composition datasets from LG-SIMS are also examined within the context of a mixed material characterization, in order to demonstrate the ability to differentiate two distinct particle endmember populations with differing isotopic contents.

3 Production and Product Characterization

3.1 Production Platform and Operations

An aerosol-based liquid-droplet to solid-particle platform was designed and assembled from a combination of commercially available and SRNL-engineered components. Key components included a Flow Focusing Monodisperse Aerosol Generator (FMAG, Model 1520, TSI Inc) for aerosol generation, an Aerodynamic Particle Sizer (APS, Model 3321, TSI Inc) for in-situ particle characterization, a diffusion dryer (Model 3062, TSI Inc), a HEPA exhaust filter, and an SRNL-designed electrostatic precipitator for aerosol collection.[10] All valve and tubing connectors are 316 stainless steel Swagelok, and all flexible connective tubing was carbon impregnated conductive silicone (TSI Inc). The aggregate system was assembled within a laboratory chemical hood approved for radiological material operations and is identified as the MPPaCS in Figure 1. The system also included a soft plastic enclosure with HEPA filter as the secondary containment to house the ESP collector.

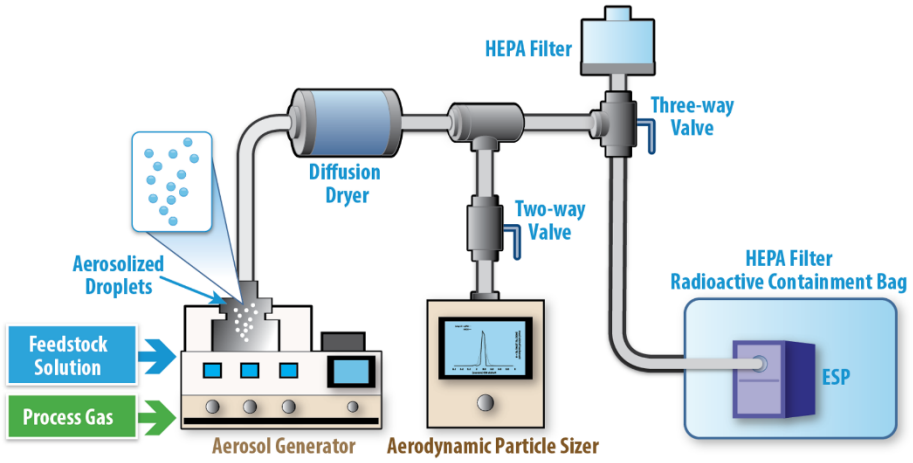

Figure 1. Schematic representation of the Monodisperse Particle Production and Collection System (MPPaCS).

All wettable components of the MPPaCS are designed for easy and rapid replacement or cleaning to minimize cross contamination between particle production operations with differing isotopic and/or elemental compositions. Disposable components include all tubing and valves, MPPaCS liquid transfer tubing, the diffusion dryer, HEPA

filters, secondary containment enclosure, and ESP. Other internal components of the FMAG and APS were cleaned between operations per vendor specified solvents to remove any retaining materials. The ESP was an engineered variant of the SRNL-developed Aerosol Contaminant Extractor (ACE) modified with an external power supply and controller to minimize electrical components in the soft plastic enclosure.[11] Disposable electropolished stainless steel plates were used as the collection media within the ESP. FMAG intake air was scrubbed by inline desiccating trap and filtered for other potential contaminants prior to intake into the MPPaCS. Uranyl oxalate feedstock solutions in ultrapure water were generated just prior to loading and were generated based on FMAG operational recommendation. Uranyl oxalate feedstocks were manufactured with standard radiochemistry methods within a separate laboratory and any unique isotopic formulations performed as previously published.[12, 13]

Typical FMAG operational parameters for production operations include orifice vibration at a 130 kHz frequency, 15.0 ± 0.1 L/min dilution air flow rate, 2.00 ± 0.05 psi flow focusing air pressure, and a 3.00 mL/h solution flow rate. These conditions were found suitable for the generation of monodisperse particulates near 1-µm, and further enabled the modification of particle size solely through changes in the uranyl oxalate concentration of the starting solution. Uranyl oxalate concentrations of 8.15×10^{-5} vol/vol were used and test specimens described in here were sourced from material with depleted uranium isotopic compositions of 0.26% or 0.17% ^{235}U. All MPPaCS operations were continually monitored by the APS to assess particle size distributions in real time and record operational stability.[14] Figure 2A shows an example of continuous operations over a 40-hour period to generate monodisperse particles with 0.82 µm average equivalent circular diameter (ECD). During operations the variance in aerodynamic size distributions was <1.15 GSD and observed drift for particle ECD average was ± 0.05 µm for the duration of operations. Aerodynamic sizing data was adjusted based on the inverse-square of the feedstock material density (3.07 g/cm^3 for uranyl oxalate) to approximate physical particle dimensions. This approximation was also correlated by modelling APS particle ECD particle size distributions scaled by density to automated particle measurements (APM) SEM measurement performed post-collection as shown in Figure 2B. The convergent overlay of the two particle histograms reaffirms the particulate average particulate density is consistent with uranyl oxalate solid.

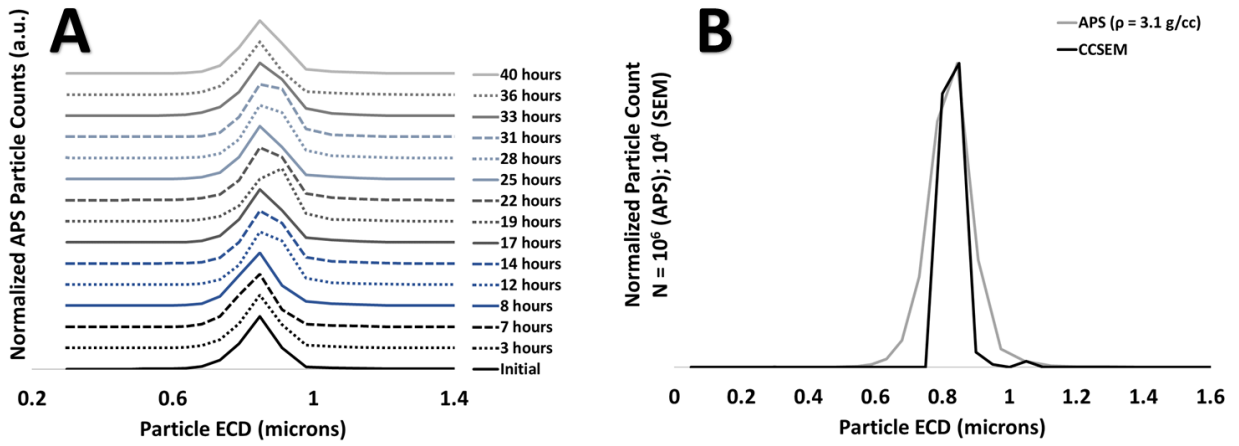

Figure 2. (A) Aerodynamic particle size profile obtained over 40 hours of MPPaCS operation, and (B) comparison of APS and APM SEM size distributions for the generated particles.

Typical MPPaCS operation durations were 10-40 hours where the dried aerosol product stream was collected onto electropolished 316 stainless steel plates via electrostatic precipitation as shown in Figure 3. The generated powders displayed a distinct yellow color, consistent with uranyl oxalate and were flowable, suggesting the MPPaCS and developed methodology were suitable for the scale-up of an aerosol-based method for QC reference particulate generation. In detail, the collection plates are extracted from the ESP, particulate material mechanically removed via a razor, and aggregated into a sample via for storage. Calculated completed conversion via MPPaCS for the uranyl oxalate solution feedstock with nominal concentration and flow rate is 0.75 mg/h. Overall laboratory production rates were lower at approximately 0.33 mg/h, which reflects a combination of incomplete ESP particle collection due to partial operational efficiency, aerosol loss during transport within the MPPaCS flow path, and material loss during the physical displacement and transfer of the powder from ESP collection plates into the storage vials. Despite these challenges a typical production operation yielded batches of particulates in 5-10 milligram aliquots as a loose powder.

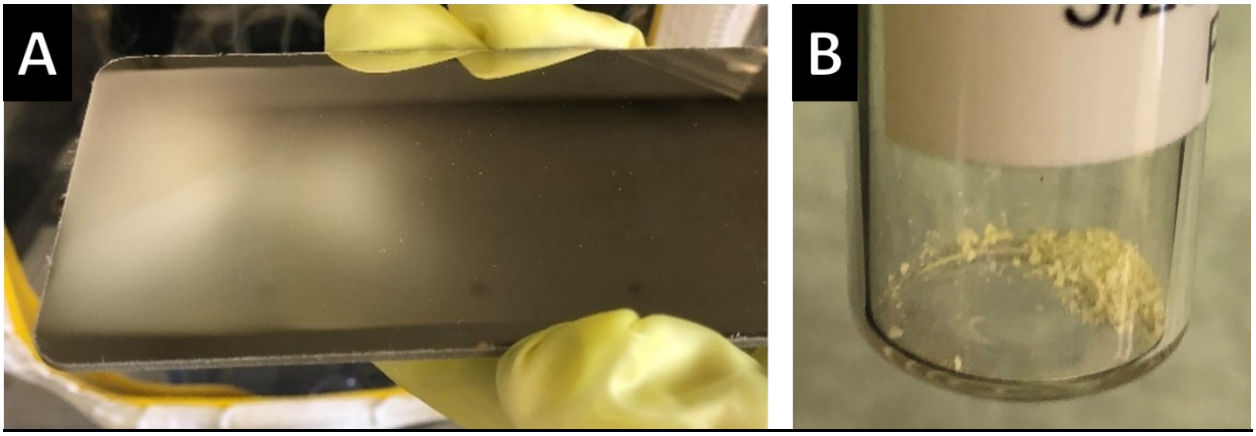

Figure 3. Optical image of particulates: (A) as-collected using electrostatic precipitation on an electropolished stainless steel plate, (B) as-harvested as loose powders.

3.2 Particulate Characterization

Uranium particulate products were characterized by a combination of analytical methods to probe both individual and particle populations to material phase, density, size (i.e., ECD), morphology, and uranium isotopic composition. APM via SEM/EDS, LG-SIMS, and APS were the primary characterization methods employed, but select Raman spectroscopy and powder XRD were performed to assess the particulates material phases. High resolution electron microscopy (Carl Zeiss Supra 40VP) of the generated particles revealed a range of particulate morphologies present, including smooth, pitted, and polycrystalline spheres as shown in Figure 4. This variance is hypothesized as the result of slight variations in the drying kinetics of the aerosolized droplets caused by minor changes in process gas conditions such as pressure, relative humidity, or temperature.[15] Despite the observed variance in morphology, the monodisperse nature of the particulates is apparent the ECD size distributions obtained from both aerodynamic and APM SEM measurements (Figure 2B), in which over 90% of particles in each batch within ± 0.05 µm of the average particle diameter, further indicated by GSDs < 1.15. The reconciliation of aerodynamic sizing with APM SEM suggest particle densities near 3.1 g/cm^3, indicating a density near that of the starting uranyl oxalate composition. The monomodal particle size distributions, combined with an understanding of the droplet-to-particle aerosol generation approach utilized, suggests that the generated particles display a high degree of interparticle mass uniformity, as required for use as QC reference materials.

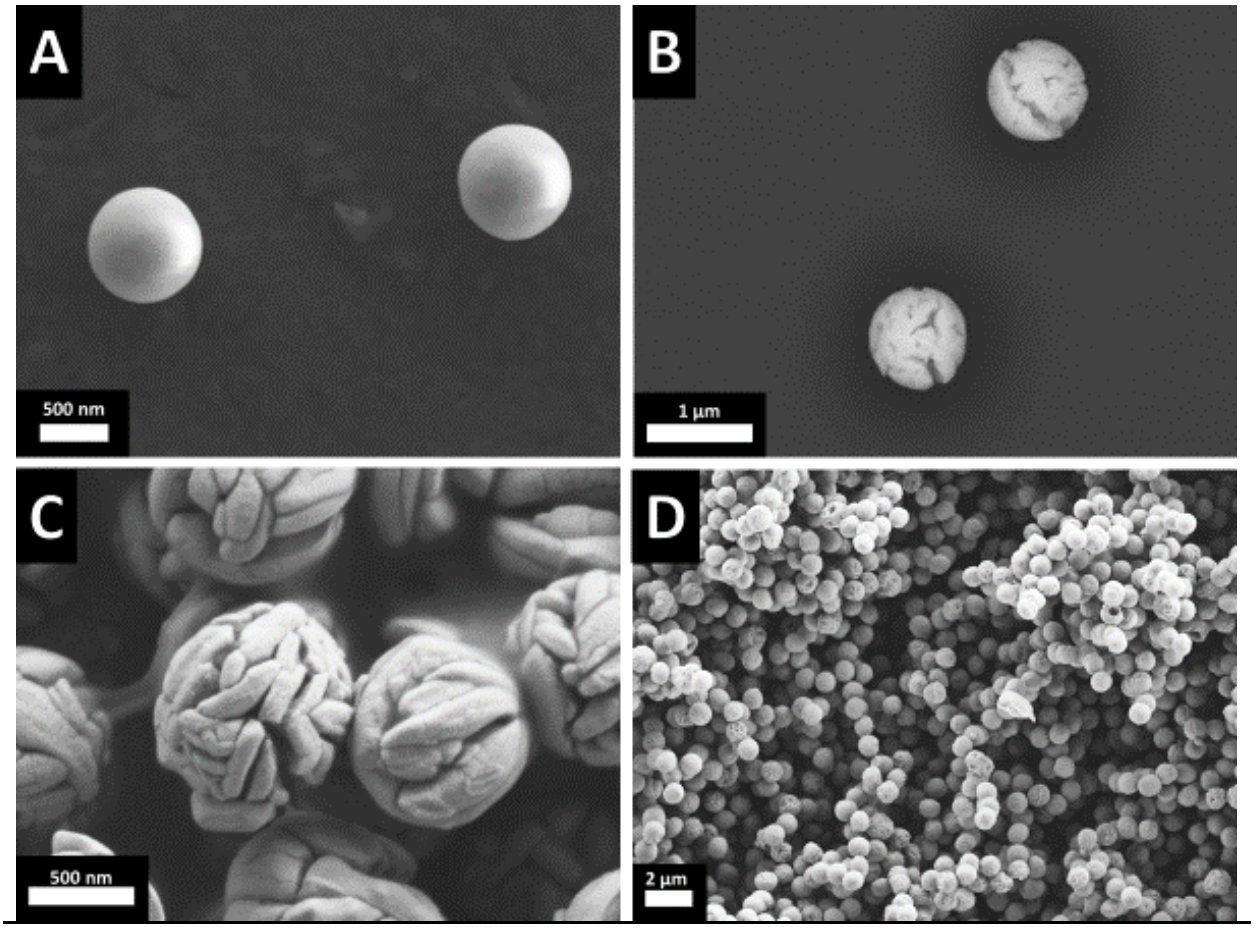

Figure 4. Comparison of the various particulate morphologies generated by the MPPaCS: (A) smooth spheres, (B) pitted spheres, (C) polycrystalline spheres, and (D) a representative milligram-scale production batch displaying a mixture of the produced morphologies.

Micro-Raman spectroscopy (LabRAM HR800 UV, Horiba Jobin–Yvon, with a λ_{ex} = 633 nm excitation laser) of multiple single particulates demonstrated intense uniform spectral features as shown in Figure 5A. All major spectra bands at 155, 204, 268, 505, 850, 921, and 1482 cm^{-1} are consistent with uranyl oxalate solids.[16] Weak spectral bands at 365, 590, and 739 cm^{-1} may represent minor phases such as those characterized by XRD, but no further attempt was made for identification. X-ray diffraction measurements (Rigaku Ultima IV) of the aggregate particulates as dry powder (Figure 5B) indicates uranyl oxalate in the major phase and with minor scan features identified as a combination of uranyl hydroxide, studtite, and metastudtite phases.[17-20] Combined, the Raman spectroscopy and XRD characterization indicates the generated particulates retain the uranyl oxalate chemistry of the feedstock material, but undergo some minor degree of chemical transformation or conversion during the aerosol-based process. The presence uranyl hydroxide, studtite, and metastudtite phases may be a sonochemical effect via the formation of hydrogen peroxide in water from operation of the FMAG ultrasonic orifice.[21, 22] Further investigation would be necessary to unambiguously characterize particle phase and any potential transformations due to the complex environmental speciation of uranium minerals.[23, 24] However, the retention of the major uranyl oxalate phase further is consistent with the calculated particle density value 3.1 g/cm^3 previously described and modelled from reconciliation of the aerodynamic and SEM particle size distributions.

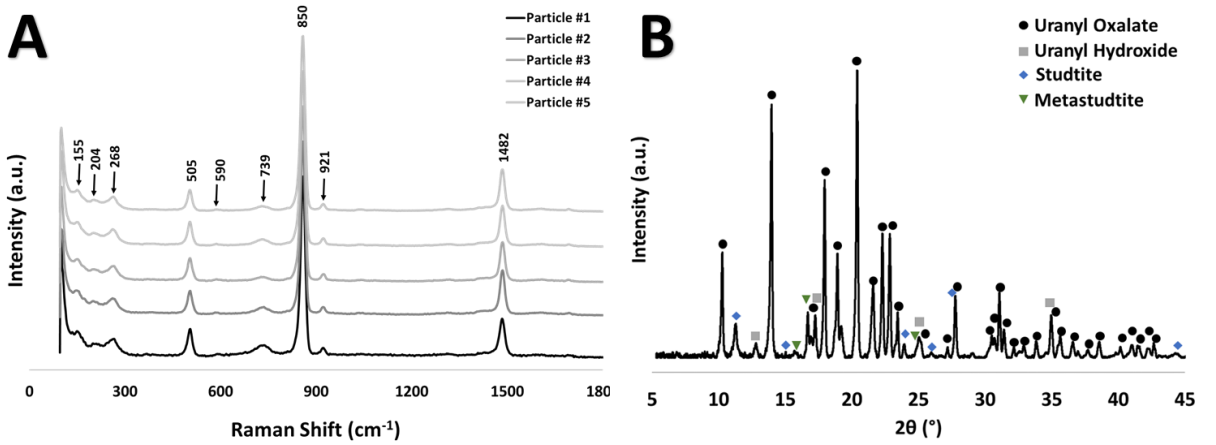

Figure 5. (A) Raman spectroscopy of MPPaCS-produced uranium-bearing particles generated via 633 nm excitation laser, and (B) X-ray diffraction scan of the MPPaCS-produced uranium-bearing particles with reflections identified by phase.

Uranium-bearing particle samples were produced from depleted uranium feedstocks with two distinct isotopic compositions and were characterized with the Los Alamos National Laboratory (LANL) Cameca IMS-1280 LG-SIMS to assess the extent of particle-to-particle isotope homogeneity for each material. Uranyl oxalate feedstocks used had DU isotope compositions with ^{235}U contents of 0.26% and 0.17% and are identified as DU-26 and DU-17, respectively. The two DU particulate materials were generated in serial, as two distinct batches, on a MPPaCS platform which was cleansed between operations. Additionally, certified reference materials (CRM)-129A and CRM-U005, representing natural and depleted uranium isotope compositions, respectively, were analyzed for comparison. The DU-26 and DU-17 samples consisted of particles dispersed across the surface of a 1" diameter carbon planchet. For each sample, two types of datasets were collected: (1) large particle populations from isotope mapping; and (2) high-precision single particle analyses; To calibrate for the SIMS instrument bias and correct unknown data, CRM U030 (3% ^{235}U) was analyzed prior to and following each sample analysis.

Map analyses were conducted through multicollection of U-isotopes. Per map analysis, a 20 nA primary ion beam was rastered over a 200 x 200 µm area. Each measurement was collected with a field aperture width of 6000 µm, an entrance slit width of 122 µm, a contrast aperture width of 400 µm and an energy slit width of 50 µm. All other secondary ion mass spectrometer (LG-SIMS) operations were performed in multi-collector mode. The ion image (map) analyses utilized optics and ion detector parameters were optimized to achieve sufficient count rates and ensure quality results. Ion map images of isotope signals were produced from five electron multiplier detectors with ^{234}U on detector L2, ^{235}U on L1, ^{236}U on C, ^{238}U on H1 and $^{238}U^{1}H$ on H2. Each map analysis duration was 240 seconds, with a prior 60 second sputter cleaning of the sample surface. For each DU sample, a 5 x 5 (or 5 x 5 grid of maps, corresponding to a 1000 x 1000 µm analysis area), was searched and located particle analyzed to generate a representative population of particles. Isotope counts per particle were determined using Cameca's Automated Particle Measurement (APM) software.[25]

Single particle measurements also employed multicollection, with identical slit and aperture settings as the APM map analyses. A primary beam raster of 10 × 10 µm was employed, with a primary beam current of 1 nA. Each particle analysis consisted of ten cycles with a 15 second dwell time per cycle, or 150 seconds of total acquisition time. Prior to analysis, each particle was pre-sputtered for 15 seconds, using a 25 µm raster and the same primary beam conditions as the analysis. For the DU-26 and DU-17 samples, twelve single particle data were collected per sample. For each sample, all single particle measurements fall within the propagated uncertainty obtained by combining: (1) the 2σ uncertainty of all particles in the dataset, and (2) the associated bias uncertainty from the instrument calibration. Good agreement of isotope compositions was obtained for the APM and single particle datasets for the MPPaCS-generated particulates, as shown in Table 1. In addition, the uncertainties of the DU-26 and DU-17 single particle data averages compare favorably with corresponding single particle measurements of CRM-129A (natural U) and CRM U005 (DU) that were collected in the same analytical session (Table 1).

Table 1. Large area secondary ion mass spectrometry results of MPPaCS-generated particulate samples for single particle [N = 12] and automated particle mapping [N = 220] measurements as compared to uranium CRMs for natural and depleted isotopic compositions.

Sample/CRM	^{234}U%	uncert. ^{234}U (%)	^{235}U%	uncert. ^{235}U (%)	^{236}U%	uncert. ^{236}U (%)	^{238}U%	uncert. ^{238}U (%)
DU-26	0.00114	0.00060	0.2624	0.0104	0.00457	0.00049	99.576	0.010
DU-26 (APM)	0.00116		0.2630		0.00423		99.732	
DU-17	0.00068	0.00035	0.1720	0.0104	0.00804	0.00086	99.640	0.010
DU-17 (APM)	0.00088		0.1733		0.00787		99.818	
CRM-129A (natural)	0.00548	0.00050	0.7429	0.0141	0.00004	0.00054	99.237	0.016
CRM U005 (depleted)	0.00216	0.00043	0.04928	0.0114	0.00469	0.00065	99.450	0.011

LG-SIMS results of MPPaCS-generated particulates were found to be isotopically homogenous within each sample. The LG-SIMS mapped datasets indicate a high-degree of particle-to-particle isotope homogeneity for the DU-27 and DU-17 materials. This determination is made by comparing (1) the total counts per particle versus their corresponding atom % values of a dataset (e.g., x and y axes, respectively, in Figure 6); and (2) a counting statistics-based model, given as the following:

$$avg.\ atom\ \% \pm \left(avg.\ atom\% \times 3.5 \times \sqrt{\frac{1}{N(avg.atom\%)_{counts}} + \frac{1}{total\,(avg.atom\%)_{counts}}} \right)$$

Where (1) $N(avg.\ atom\%)$ is the counts of the U isotope of interest; and (2) $total(avg.\ atom\%)$ is the total counts, that correspond to the average atom percent value of a particle dataset. By applying various count combinations of $N(avg.\ atom\%)$ and $total(avg.\ atom\%)$, model curves are generated that predict the scatter of particle data for a specified *avg. atom%* value in the equation above and are expressed as the red and blue curves in Figure 6. In the model, the numerical term 3.5 is a factor related to the proportion of data falling within the envelope, much like a probability distribution. For example, when values of this factor are lower, the model envelope pinches together, meaning fewer data plot within the envelope; if the factor is 2 (instead of 3.5), approximately 95 percent of data plot within the model envelope; if the factor is 1, approximately 66 % of data plot within the model envelope. This behavior approximates a normal distribution function, meaning that a value of 3.5 should correspond to 99 %+ of data plotting within the model envelope. This value was purposefully chosen for the model, in order to minimize apparent outliers that actually represent scatter of particle data that are isotopically homogeneous. For reference, this model has been applied to several particle datasets from uranium CRMs with a wide range of isotope compositions, and, assuming these materials are homogeneous, the model accurately reproduces the isotope compositional scatter as a function of counts per particle.

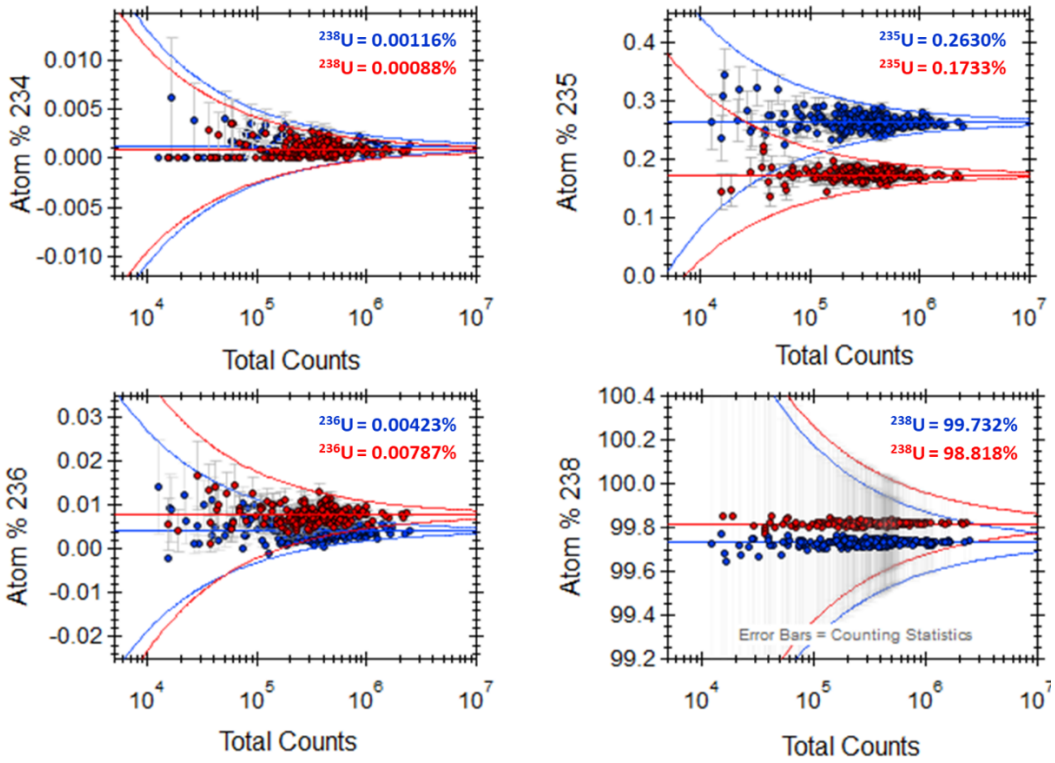

Figure 6. Example LG-SIMS mapped isotope data overlays for DU-26 and DU-17 (blue and red data respectively), as atom percent (A) ^{234}U, (B) ^{235}U, (C) ^{236}U and (D) ^{238}U versus total counts [n = 220]. The blue and red horizontal lines represent the calculated average of the DU-26 and DU-17 datasets, and curved blue and red lines are the predicted models of data scatter for the DU-26 and DU-17 averaged values (respectively) if the datasets are isotopically homogeneous (see the equation in the main text).

Figure 6 displays the comparison of the LG-SIMS APM results for the MPPaCS-produced particles generated from the DU-17 and DU-26 uranium feedstocks as data overlays. When compared to respective models of data scatter, the LG-SIMS APM mapping data have no measured outliers about the averaged DU-26 and DU-17 isotope compositions. This indicates that within the precision of the LG-SIMS map analyses, the particle populations are isotopically homogeneous within a batch. Furthermore, if one considers a hypothetical QC testing scenario in which a material consists of mixed DU-26 and DU-17 particulates, the LG-SIMS single particle and APM mapping measurements would be able to discriminate these endmembers based on their ^{235}U and ^{238}U contents, but ^{234}U would be statistically undistinguishable (Table 1 and Figure 6); APM of atom percent ^{236}U compositions would likely fail to differentiate between the two source materials (Figure 6) but single particle analyses would be successful as DU-26 (^{236}U at% = 0.00457; 0.00049 SD) is sufficiently distinct from DU-17 (^{236}U at% = 0.00804; 0.00086 SD).

4 Conclusion

A platform has been developed and demonstrated the capability to produce uranium-bearing microparticulates at the milligram-scale via aerosol-based synthesis methods. The products are primarily a uranyl oxalate phase, possess monodisperse-sized particle populations, and have homogeneous interparticle uranium isotope compositions. Refinements of the production parameters allow the generation of fit-for-purpose reference particulates within a range of particle sizes and isotopic compositions suitable for NWAL QC needs. Future development efforts will include further MPPaCS engineering to enable synthesis oxide phase particulates using inline thermal conversion, generation of mixed actinide reference particulates (e.g., U/Th and U/Pu), and modifications to allow tailored particle collections on substrates.

5 Acknowledgements

The authors wish to thank the team at the IAEA Safeguards Analytical Laboratory, and David Simons and Todd Williamson from US National Institute of Science and Technology for their expert advice and critical feedback throughout this work. This work was produced by Savannah River National Laboratory (Battelle Savannah River Alliance, LLC) and by Los Alamos National Laboratory (Triad National Security, LLC) under Contracts No. 89303321CEM000080 and 89233218CNA000001, respectively, with the U.S. Department of Energy. This work was sponsored by the National Nuclear Security Administration of the Department of Energy, Office of International Nuclear Safeguards – Safeguards Technology Development program. Publisher acknowledges the U.S. Government license to provide public access under the DOE Public Access Plan (http://energy.gov/downloads/doe-public-access-plan).

6 References

1. IAEA, Research and Development Plan: STR-385. In Safeguards, I., Ed. IAEA: Vienna AU, January 2018.
2. IAEA, Development and Implementation Support Programme for Nuclear Verification 2020—2021 STR-393. In Safeguards, I., Ed. IAEA: Vienna AU, January 2020.
3. Pope, T. R.; Arey, B. W.; Zimmer, M. M.; DeVore, I.; Bronikowski, M. G.; Kuhne, W.; Baldwin, A. T.; Padilla Cintron, C.; Anheier, N. C.; Warner, M. G. *Production of Particle Reference and Quality Control Materials*; Pacific Northwest National Lab.(PNNL), Richland, WA (United States): 2019.
4. Trillaud, V.; Maynadie, J.; Manaud, J.; Hidalgo, J.; Meyer, D.; Podor, R.; Dacheux, N.; Clavier, N., Synthesis of size-controlled UO 2 microspheres from the hydrothermal conversion of U (iv) aspartate. *CrystEngComm* **2018,** *20*, (48), 7749-7760.
5. Neumeier, S.; Middendorp, R.; Knott, A.; Dürr, M.; Klinkenberg, M.; Pointurier, F.; Sanchez, D. F.; Samson, V.-A.; Grolimund, D.; Niemeyer, I., Microparticle production as reference materials for particle analysis methods in safeguards. *MRS Advances* **2018,** *3*, (19), 1005-1012.
6. Venchiarutti, C.; Richter, S.; Middendorp, R.; Aregbe, Y., NUSIMEP-9: Uranium isotope amount ratios and uranium mass in uranium micro-particles. **2019**.
7. Truyens, J.; Dürr, M.; Macsik, Z.; Middendorp, R.; Neumeier, S.; Richter, S.; Stadelmann, G.; Venchiarutti, C.; Aregbe, Y., IRMM-2329P. **2020**.
8. Kegler, P.; Pointurier, F.; Rothe, J.; Dardenne, K.; Vitova, T.; Beck, A.; Hammerich, S.; Potts, S.; Faure, A.-L.; Klinkenberg, M., Chemical and structural investigations on uranium oxide-based microparticles as reference materials for analytical measurements. *MRS advances* **2021,** *6*, (4), 125-130.
9. Truyens, J.; Neumeier, S.; Kegler, P.; Klinkenberg, M.; Zoriy, M.; Richter, S.; Aregbe, Y., Preparation and Certification of the Uranium Oxide Micro Particle Reference Material IRMM-2331P. **2021**.
10. Duan, H.; Romay, F. J.; Li, C.; Naqwi, A.; Deng, W.; Liu, B. Y., Generation of monodisperse aerosols by combining aerodynamic flow-focusing and mechanical perturbation. *Aerosol Science and Technology* **2016,** *50*, (1), 17-25.
11. Carlson, D. C.; Degange, J. J.; Cable-Dunlap, P., Portable aerosol contaminant extractor. In Google Patents: 2005.
12. Baldwin, A. T.; Wellons, M. S., Applicability of Targeted Actinide Reference Materials to Fuel Cycle Safeguards - Doc# SRNS-STI-2020-00289. In SRNL: 2020.
13. Barrett, C. A.; Pope, T. R.; Arey, B. W.; Zimmer, M. M.; Padilla -Cintron, C.; Anheier, N. C.; Warner, M. W.; Baldwin, A. A. T.; Bronikowski, M. G.; DeVore II, M.; Kuhne, W.; Wellons, M. S. In *Production of Particle Reference and Quality Control Materials*, 41st ESARADA Conference December 2019, 2019; 2019; pp 29-38.
14. Chen, B.; Cheng, Y.; Yeh, H., Performance of a TSI aerodynamic particle sizer. *Aerosol science and technology* **1985,** *4*, (1), 89-97.
15. Knott, A.; Roth, G.; Bosbach, D., *Production and characterization of monodisperse uranium particles for nuclear safeguards applications*. Fachgruppe für Rohstoffe und Entsorgungstechnik: 2017.
16. Kampf, A. R.; Plášil, J.; Nash, B. P.; Němec, I.; Marty, J., Uroxite and metauroxite, the first two uranyl oxalate minerals. *Mineralogical Magazine* **2020,** *84*, (1), 131-141.
17. Jayadevan, N.; Chackraburtty, D., The crystal and molecular structure of uranyl oxalate trihydrate. *Acta Crystallographica Section B: Structural Crystallography and Crystal Chemistry* **1972,** *28*, (11), 3178-3182.
18. Peters, J., *Synthese et etude radiocristallographique d'uranates synthetiques du type oxyde double d'uranyle*. Presses Acad. Europeennes: 1967.

19. Guillemin, C. L.; Destas, A.; Vaes, J., *Minéraux d'uranium du Haut Katanga*. Les Amis du Musée Royal du Congo Belge: 1958.
20. Debets, P., X-ray diffraction data on hydrated uranium peroxide. *Journal of Inorganic and Nuclear Chemistry* **1963,** *25*, (6), 727-730.
21. Anbar, M.; Pecht, I., On the sonochemical formation of hydrogen peroxide in water. *The Journal of Physical Chemistry* **1964,** *68*, (2), 352-355.
22. Ziembowicz, S.; Kida, M.; Koszelnik, P., The impact of selected parameters on the formation of hydrogen peroxide by sonochemical process. *Separation and Purification Technology* **2018,** *204*, 149-153.
23. Kirkegaard, M. C.; Niedziela, J. L.; Miskowiec, A.; Shields, A. E.; Anderson, B. B., Elucidation of the structure and vibrational spectroscopy of synthetic metaschoepite and its dehydration product. *Inorganic chemistry* **2019,** *58*, (11), 7310-7323.
24. Spano, T. L.; Niedziela, J. L.; Shields, A. E.; McFarlane, J.; Zirakparvar, A.; Brubaker, Z.; Kapsimalis, R. J.; Miskowiec, A., Structural, Spectroscopic, and Kinetic Insight into the Heating Rate Dependence of Studtite and Metastudtite Dehydration. *The Journal of Physical Chemistry C* **2020,** *124*, (49), 26699-26713.
25. Peres, P.; Hedberg, P.; Walton, S.; Montgomery, N.; Cliff, J.; Rabemananjara, F.; Schuhmacher, M., Nuclear safeguards applications using LG-SIMS with automated screening capabilities. *Surface and interface analysis* **2013,** *45*, (1), 561-565.